

A long-period massive planet around HD106515A *

S. Desidera¹, R. Gratton¹, E. Carolo^{1,2}, A.F. Martinez Fiorenzano³, M. Endl⁴, D. Mesa¹, M. Cecconi³, R. Claudi¹, R. Cosentino^{3,5}, S. Scuderi⁵, A. Sozzetti⁶, A. Zurlo^{1,7}

¹ INAF – Osservatorio Astronomico di Padova, Vicolo dell' Osservatorio 5, I-35122, Padova, Italy

² Dipartimento di Astronomia – Università di Padova, Vicolo dell'Osservatorio 2, Padova, Italy

³ INAF – Centro Galileo Galilei, Calle Alvarez de Abreu 70, 38700 Santa Cruz de La Palma (TF), Spain

⁴ McDonald Observatory, The University of Texas at Austin, Austin, TX 78712, USA

⁵ INAF – Osservatorio Astrofisico di Catania, Via S.Sofia 78, Catania, Italy

⁶ INAF – Osservatorio Astrofisico di Torino, via Osservatorio 20, 10025 Pino Torinese, Italy

⁷ Aix Marseille Université, CNRS, LAM (Laboratoire d'Astrophysique de Marseille) UMR 7326, 13388, Marseille, France

Received / Accepted

ABSTRACT

We have performed RV monitoring of the components of the binary system HD 106515 over about 11 years using the high resolution spectrograph SARG at TNG. The primary shows long-period radial velocity variations that indicate the presence of a low mass companion whose projected mass is in the planetary regime ($m \sin i = 9.33 M_J$). The 9.8 years orbit results quite eccentric ($e = 0.57$), as typical for massive giant planets. Our results confirm the preliminary announcement of the planet included in Mayor et al. (2011). The secondary instead does not show significant RV variations. The two components do not differ significantly in chemical composition, as found for other pairs for which one component hosts giant planets. Adaptive optics images obtained with AdOpt@TNG do not reveal additional stellar companions. From the analysis of the relative astrometry of the components of the wide pair we put an upper limit on the mass of the newly detected companion of about $0.25 M_\odot$. State of art or near future instrumentation can provide true mass determination, thanks to the availability of the wide companion HD106515B as reference. Therefore, HD106515Ab will allow deeper insight in the transition region between planets and brown dwarfs.

Key words. (Stars:) individual: HD 106515 - Planetary systems - (Stars:) binaries: visual - Techniques: spectroscopic - (Stars:) brown dwarfs - Techniques: high angular resolution

1. Introduction

The upper mass limit of planetary objects is currently widely debated in the scientific community. On one hand, an operational definition can be based on the minimum mass for deuterium burning (about $13 M_J$) as a dividing line between planets and brown dwarfs (Burrows et al. 2001), as defined by IAU (Boss et al. 2012), or to different fixed threshold values (e.g. $24 - 25 M_J$: Butler et al. 2006; Schneider et al. 2011). On the other hand, a definition based on formation mechanisms is more difficult to obtain. In fact, observational data are incomplete and the detection techniques in most cases can provide only indirect indication on the formation of a detected substellar objects. Furthermore, only minimum masses are known for most of the objects detected by RV surveys or, in the case of objects detected through direct imaging, true masses are uncertain because of the large sensitivity of luminosity on age and intrinsic uncertainties of theoretical models especially at young ages (Baraffe et al. 2003).

Send offprint requests to: S. Desidera,
e-mail: silvano.desidera@oapd.inaf.it

* Based on observations made with the Italian Telescopio Nazionale Galileo (TNG) operated on the island of La Palma by the Fundacion Galileo Galilei of the INAF (Istituto Nazionale di Astrofisica) at the Spanish Observatorio del Roque de los Muchachos of the Instituto de Astrofisica de Canarias.

In spite of these difficulties there is growing evidence for a significant overlap in mass between objects formed like stars do and objects formed in a protoplanetary disks. Several objects of planetary mass have been detected as free floating objects in star clusters, star forming regions or in the field using imaging (e.g. Zapatero Osorio et al. 2000; Leggett et al. 2012; Scholz et al. 2012) and microlensing (Sumi et al. 2011) or as very wide companions of stars (e.g. Chauvin et al. 2005). Some of these objects might be formed in planetary systems and then pushed at very wide separation or ejected from the system because of dynamical interactions with other planets (Jumping Jupiters scenario, Marzari & Weidenschilling 2002). However, it seems unlikely this is the only mechanism producing free floating objects below deuterium burning mass (Bowler et al. 2011). Instead, the minimum mass for core collapse was found to be of a few M_J and is then likely that objects of planetary mass formed star-like outside planetary disks (Whitworth et al. 2007). The statistics of low mass brown dwarfs appear to be compatible with Jeans mass fragmentation of an interstellar molecular cloud (Zuckerman & Song 2009).

On the other hand, there are objects with masses from 13 to about $25 M_J$ that are found in systems with other lower mass planets, such as HD168443 and HAT-P13. In the latter case the planetary nature of the lower mass companion is confirmed by the occurrence of transits (Bakos et al.

2009). In other cases such as HD 38519 and HD 202206 a debris disk is present in the system beside a massive planet and a lower mass planet (Moro-Martín et al. 2010). These facts support the formation of these objects in a protoplanetary disks. Planet formation models also predict the presence of very massive planets, up to about $38 M_J$, in exceptional cases of long-lived, massive and metal-rich disks (Mordasini et al. 2009). The rising mass function below about $20 - 30 M_J$ (Grether & Lineweaver 2006) is another indication that a different formation mechanism starts to be present above deuterium burning mass.

This picture is further complicated by evidences that the statistical properties of planetary mass companions with (projected) masses between 4 to $15 M_J$ are different from those of lower mass planets (Ribas & Miralda-Escudé 2007). It is then possible that either a different formation mechanism is in action or that the evolution of massive planets in a protoplanetary disk is different depending on planetary mass.

The statistic of substellar objects in the mass range between 10 to $30 M_J$ is still limited, given the intrinsic rarity of these objects (Sozzetti & Desidera 2010; Díaz et al. 2012). The discovery of additional candidates is then welcome, especially when the true mass of the companion can be determined or significantly constrained through astrometry (Sahlmann et al. 2011; Reffert & Quirrenbach 2011). We present here the confirmation of a high-mass planet candidate orbiting the star HD106515A and clues on its mass from astrometry. The planet was first included in the compilation by Mayor et al. (2011) but only orbital period, RV semiamplitude, eccentricity, and corresponding minimum masses and semimajor axis are listed, postponing a more detailed analysis to a forthcoming paper. HD 106515A is part of a wide binary system, with the companion HD 106515B at a projected separation of about 250 AU. Both components were observed as part of the RV survey looking for planets around the components of moderately wide binaries performed using SARG at TNG.

2. Observations and data reduction

Observations were performed at the Italian Telescopio Nazionale Galileo (TNG) using the high resolution spectrograph SARG (Gratton et al. 2001). All but one spectra, used as template in the RV determination process, were acquired with the iodine cell inserted in the optical path. The observing procedure and the instrument set-up are the standard ones for SARG planet search survey. We refer to Desidera et al. (2011) for further details. In the case of HD106515, the chance of contamination of the spectra is negligible even in the worst observing conditions, thanks to the 6.8 arcsec separation on the sky between the components.

The acquisition of data on HD106515 was stopped after May 2009 because of lack of time allocation and was recently restarted after the publication of Mayor et al. (2011), that listed a planet around the primary component of this system. The 900s integration yields typical S/N ratios of 100. for HD106515A and 90 for HD106515B.

Differential radial velocities were obtained using the AUSTRAL code (Endl et al. 2000), achieving internal errors of about 3 m/s. Data taken in 2011-2012 have a somewhat larger uncertainty, because of significant asymmetries

of the spectrograph instrument profile. Standard RV analysis performed using a central Gaussian with two or four Gaussian satellites show RV higher by few tens of m/s with respect to previous data. However, when analyzing the data exploiting the Maximum Entropy algorithm such discrepancy vanishes. In any case, while the internal errors are similar to the older data, we can not exclude the occurrence of systematics at 10-15 m/s level for these recent data. The RV time series of HD106515A and B are reported in Table 3 and 4.

HD 106515 was also observed on 21 June 2007 using AdOpt@TNG (Cecconi et al. 2006). At that time only a long term trend was appearing from RV data and our observations were aimed at the direct detection of the companion responsible for the trend. The acquisition and data reduction procedures are the same as done for HD132563 in Desidera et al. (2011), with the differences that all the images on HD106515 were taken using the broad band K' filter and at the same rotation angle. 194 images were acquired and used in our analysis. The projected separation between HD106515 A and B results of 6.897 ± 0.015 arcsec and the position angle of 267.07 ± 0.12 deg. Detection limits in K band magnitude difference were transformed in mass limits using the mass-luminosity relation by Delfosse et al. (2000) at $M_K < 9.5$ and the 5 Gyr theoretical isochrone by Chabrier et al. (2000) at fainter magnitudes.

3. Stellar properties

HD 106515 (HIP 59743, GJ 9398, ADS 8477) is a pair formed by two similar stars slightly less massive than the Sun. The main properties of the components of HD 106515 are summarized in Table 1.

The metallicity of the components was studied by us using both SARG and FEROS spectra (Desidera et al. 2004, 2006a). The metallicity resulted close to solar. The line-by-line abundance differential analysis did not reveal significant abundance difference between the components.

The slow projected rotational velocity, low level of chromospheric activity (Desidera et al. 2006a; Gray et al. 2003; Arriagada 2011), and lack of detection in ROSAT All Sky Survey (Voges et al. 2000) are all consistent with a rather old age, at least as old as the Sun. Isochrone fitting does not allow to put firm constraints on stellar age, because of long timescales of the evolution of stars less massive than the Sun. The thin disk kinematic places an upper limit of about 8 Gyr. The system age is then in the range between 4 to 8 Gyr.

4. A massive planet around HD106515

The RV time-serie of HD 106515A shows a long period modulation clearly detectable by eye (Fig. 1). Lomb-Scargle periodogram confirms the long periodicity and the lack of shorter periodicities in the data. The low level of chromospheric activity guarantees the Keplerian origin of the RV variations observed for HD 106515A. An expected activity jitter of 3.5 m/s was derived using Wright (2005) calibration. We then performed Keplerian fitting using a Levenberg-Marquardt least-squares fit algorithm as in Desidera et al. (2011). The parameters are similar to those derived by Mayor et al. (2011). Both orbital parameters are listed in Table 2. The residuals from the best fit Keplerian

Table 1. Stellar properties of the components of HD 106515.

Parameter	HD 106515 A	HD 106515 B	Ref.
α (2000)	12 15 06.567	12 15 06.103	1
δ (2000)	-07 15 26.38	-07 15 26.61	1
μ_α (mas/yr)		-249.67 ± 0.91	2
μ_δ (mas/yr)		-52.29 ± 0.74	2
RV (km/s)	20.66 ± 0.11	19.94 ± 0.11	3
π (mas)		28.42 ± 0.96	2
d (pc)		35.2 ± 1.1	2
U (km/s)		-28.0	4
V (km/s)		-38.7	4
W (km/s)		4.6	4
V	7.960 ± 0.005	8.234 ± 0.007	5
ΔV		0.272 ± 0.003	5
B-V		0.815 ± 0.003	1
B-V	0.793 ± 0.021	0.830 ± 0.034	5
V-I		0.83 ± 0.02	1
H_p scatter		0.011^a	1
J_{2Mass}	6.585 ± 0.024	6.746 ± 0.030	6
H_{2Mass}	6.218 ± 0.046	6.362 ± 0.034	6
K_{2Mass}	6.151 ± 0.026	6.267 ± 0.017	6
NUV magnitude		14.02	7
FUV magnitude		-	7
T_{eff} (K)	5232	5073	5
$\Delta T_{eff}(A - B)$ (K)		164 ± 21	5
$\log g$	4.31	4.32	5
$\log R'_{HK}$	-5.04	-5.07	3
$\log R_{HK}$	-5.07		8
$\log R_{HK}$	-5.06	-5.04	9
$v \sin i$ (km/s)	0.6	1.3	3
[Fe/H]	0.01	0.00	5
$\Delta[\text{Fe}/\text{H}](A - B)$		0.009 ± 0.017	5
Mass(M_\odot)	0.91 ± 0.03^b	0.88 ± 0.03^b	4
Age (Gyr)		$\sim 4 - 8$	4

References: 1 Hipparcos (Perryman & ESA 1997); 2 van Leeuwen (2007); 3 Desidera et al. (2006b); 4 This Paper; 5 Desidera et al. (2006a); 6 2MASS (Skrutskie et al. 2006); 7 Galex (Martin et al. 2005); 8 Gray et al. (2003); 9 Arriagada (2011)

^a A+B

^b Derived using the PARAM web interface (da Silva et al. 2006)

orbit have an rms of about 6 m/s, and the periodogram does not show indication of additional significant periodicities (Fig. 2). We then conclude that HD 106515A is orbited by a companion whose minimum mass is in the planetary regime. This should then be identified as HD 106515Ab. In the following section we will exploit the available astrometric data to further constrain the mass of the companion.

The RV curve of the wide companion HD 106515B shows instead a scatter only slightly larger than internal errors (rms 8.7 m/s), without significant periodicities or long term trends (Fig. 3).

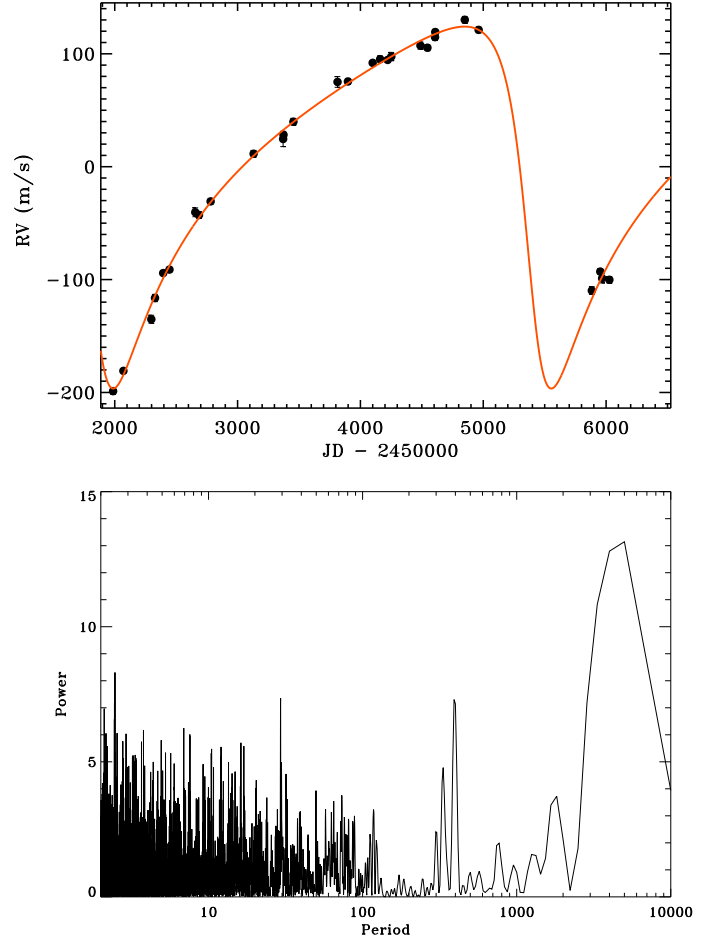

Fig. 1. Upper panel: radial velocities of HD 106515A. Overplotted the Keplerian best fit. Lower panel: Lomb-Scargle periodogram of the radial velocities.

Table 2. Orbital parameters and results of fitting for RV of HD106515A.

Parameter	Our fit	Mayor et al. 2011
Period (d)	3567 ± 14	3630
K (m/s)	160 ± 3	174
e	0.57 ± 0.01	0.60
ω (deg)	124 ± 14	-
T0 (JD-2450000)	1844 ± 27	-
$m \sin i$ (M_J)	9.33 ± 0.16	10.50
a (AU)	4.43 ± 0.01	-
rms res (m/s)	6.0	-

5. Search for astrometric signature

Considering the parameters from the RV orbit and the distance to the system, the amplitude of the astrometric signature for the RV minimum mass is about 1.2 mas. While we do not expect to be able to detect such astrometric motion in current data, it is possible to have a significant detection in case the orbit is seen close to pole-on and the actual mass is significantly larger than the projected mass.

We considered all the relative astrometry measurements available in Washington Double Star catalog (kindly provided by B. Mason), that span about 180 yr. Long period

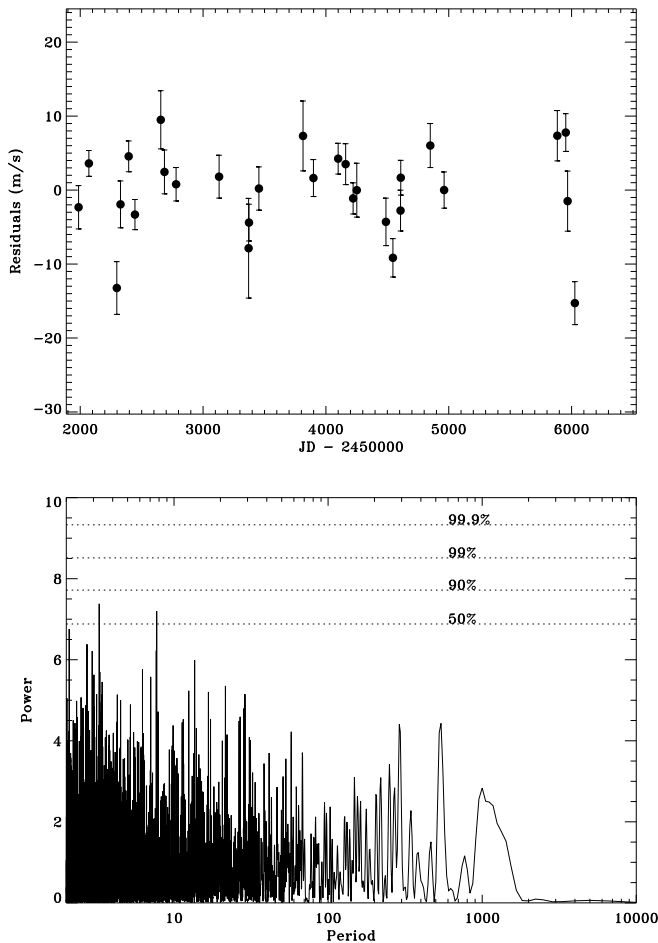


Fig. 2. Upper panel: Residuals from best fit orbit vs time Lower panel: Lomb-Scargle periodogram of residuals from the Keplerian best fit of the radial velocities of HD106515A, with false alarm probability levels from bootstrap simulation overlotted.

trends are clearly seen in both position angle and projected separation, as expected from the orbital motion of the wide pair (Fig. 4). The observed slopes will be used in Sect. 6 to constrain the binary orbit. Short term slopes as measured with Hipparcos are consistent with those based on the full dataset, supporting the lack of additional high amplitude astrometric perturbations on the timescales comparable to the mission lifetime.

Residuals from long term quadratic slope show a much larger scatter before 1930 (Fig. 5). We therefore considered only data taken after 1930 for the search of astrometric signatures due to the RV companion. Lomb Scargle periodograms of residuals in X and Y coordinates have very low power at period close to that of RV orbit. A possible periodicity is revealed at about 70 yr, especially in Y coordinate (the modulation can also be seen by eye in the projected separation vs time plot). Given the dense sampling of the astrometric measurements, this periodicity should not be related to the RV companion.

If we limit our analysis to data from USNO (Franz 1963; Kallarakal et al. 1969; Josties et al. 1978) and Heintz (1987) (Fig. 7), to have a more homogeneous dataset and reduce the impact of absolute calibration errors that might

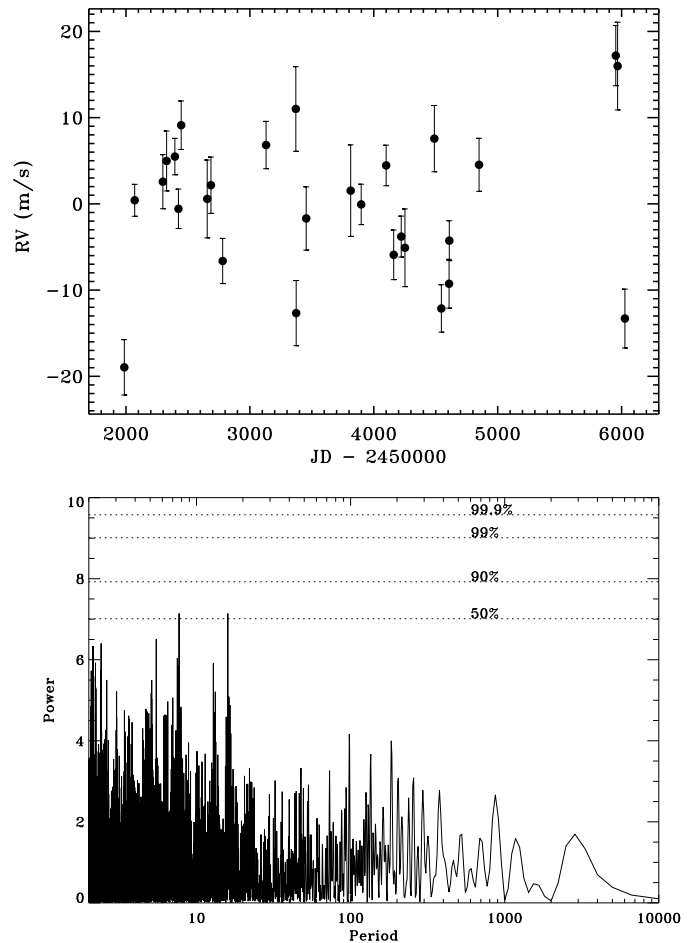


Fig. 3. Upper panel: RV time serie of HD106515B Lower panel: Lomb-Scargle periodogram of RVs and false alarm probability levels from bootstrap simulation.

be present when using different instrumentation, we have that the residuals have a dispersion of 13 mas in X and 20 mas in Y, and of 14 and 15 mas in X and y respectively when taking the 70yr periodicity mentioned above into account. These data cover 22 years. We then estimate an upper limit on the astrometric amplitude with 10 yr period of about 30 mas, comparing the expected astrometric motion of the companion for different masses with the USNO and Heintz (1987) dataset. This corresponds to a limit in mass of about $0.25 M_{\odot}$.

The tentative 70 yr periodicity with its possible amplitude of about 50 mas would correspond to a very low mass star of about $0.1 M_{\odot}$. The corresponding semimajor axis would be of about 17 AU, i.e. 0.5 arcsec on the sky. Our images taken with AdOpt@TNG do not reveal stellar companions with masses larger than $0.15 - 0.2 M_{\odot}$ at such a projected separation either around HD106515A or around HD106515B (Fig. 8), therefore, the non-detection is not conclusive. The RV semiamplitude of a $0.1 M_{\odot}$ companion in 70yr orbit in edge-on circular orbit is about 700 m/s, with RV difference that might reach 600 m/s over 10 years. The real slope might be significantly smaller than this value, depending on the actual phase of the orbit at the time of the observations, inclination, eccentricity. The data of HD106515B does not reveal significant long term

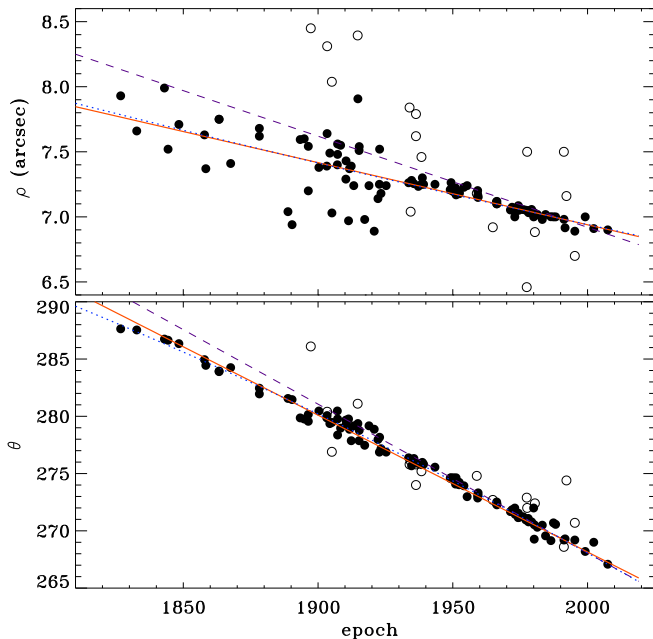


Fig. 4. Upper panel: projected separation vs time for HD106515. Bottom panel: position angle vs time. In both panels filled circles are the measurements kept in the fit and the empty circles are those removed as being outliers in either projected separation or position angle. In both panels, red continuous line is the linear fit imposing passage through Hipparcos measurement, blue dotted line is the quadratic fit, purple dashed line is the slope as measured from Hipparcos (baseline 3.25 yr; epoch 1991.25) extrapolated to the whole baseline of available data.

trends (Fig. 3), making very unlikely that such an additional companion is orbiting around this star. The RV data for HD106515A are less adequate for the study of additional long term trends as the temporal baseline slightly exceeds one orbital period of HD106515Ab and the sampling after 2009 is poor. Nevertheless, we do have specific indications of the presence of an additional long term trend in the data.

We also note that no measurable differences are found in the stellar proper motion between the new reduction of the short-term Hipparcos astrometric data for HD 106515 (van Leeuwen 2007) and the long-term Tycho-2 data (Høg et al. 2000). The proper motion values in the two catalogs agree well with each other within the quoted uncertainties, thus no useful constraint can be obtained on the orbit and mass ratio based on the $\Delta\mu$ technique (e.g. Makarov & Kaplan 2005).

6. Binary orbit

To constrain the orbit of the HD106515 system, we considered the long term relative astrometry (Sect. 5) and the RV difference between the components. To derive this latter quantity, we measured the radial velocities of both components using the stellar template of HD106515A. Taking the orbital motion of the massive planet around the primary into account, such a difference results of $\Delta RV_{A-B} = 739$ m/s. Internal errors derived from the error of the mean of the RV of the individual components and number of spec-

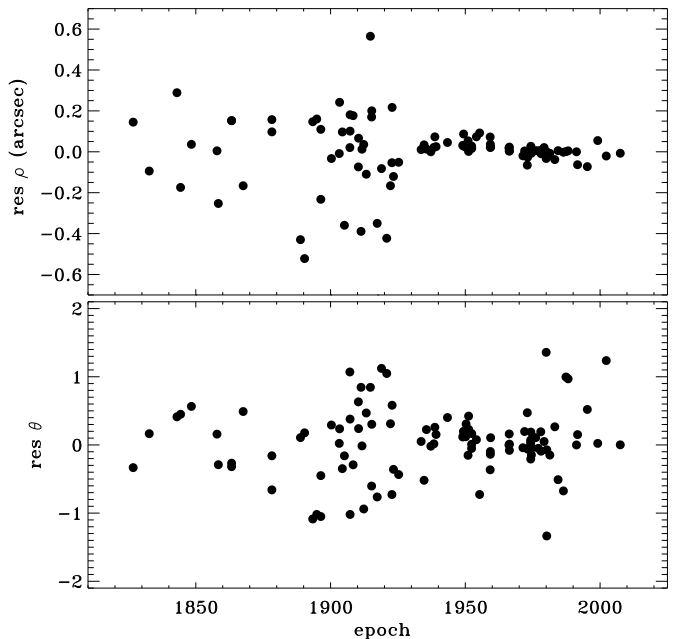


Fig. 5. Residuals from quadratic fit in Fig. 4. Upper panel: projected separation. lower panel: position angle.

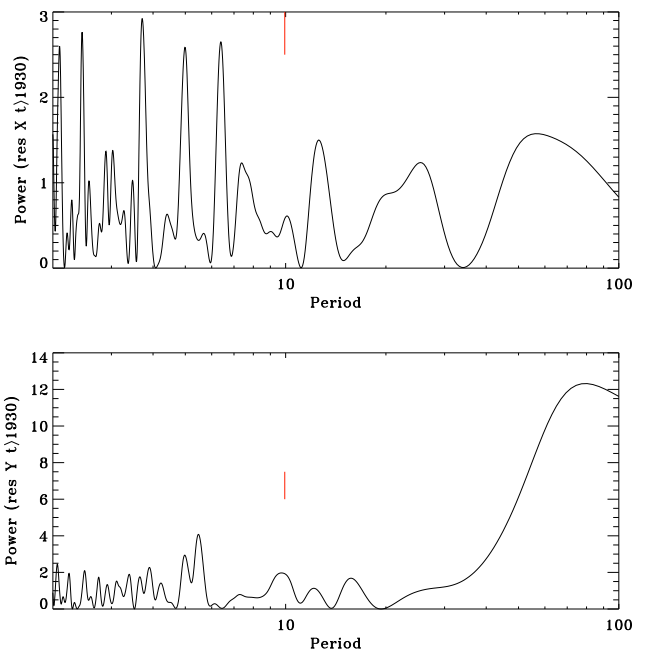


Fig. 6. Lomb-Scargle periodogram of the residuals from full-data quadratic fit in X and Y coordinates. Only data after 1930 were considered because of their higher precision. The short vertical lines at 10yr mark the RV period.

tra and including uncertainty in the planet orbit are within 10 m/s. Systematic effects due to spectral mismatch were estimated by Nidever et al. (2002) to be of the order of 100 m/s when using solar spectrum as template for the derivation of the absolute RVs of FGK stars. This effect would be significantly smaller in our case thanks to the small temperature difference between the components and the very

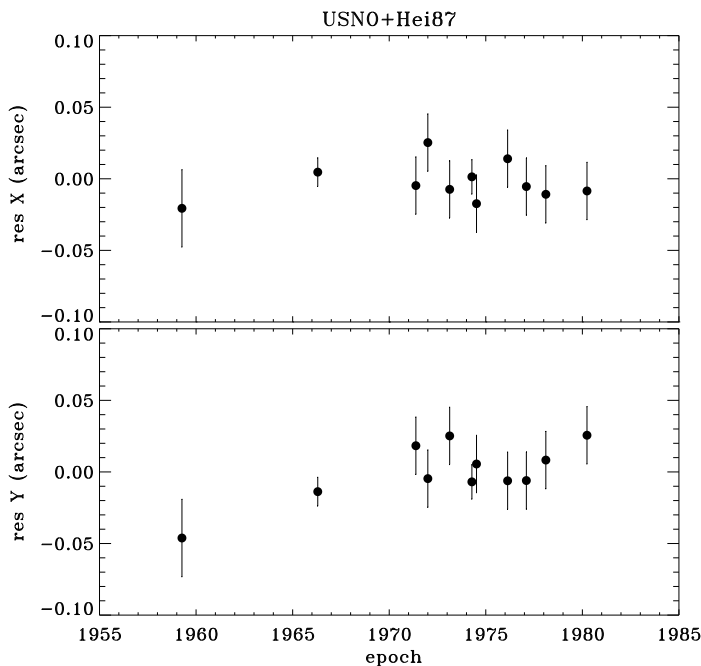


Fig. 7. Residuals from full-data quadratic fit in X and Y coordinates. Only data from USNO (yearly averages) and Heintz 1987 are shown.

similar metallicities and projected rotational velocities. The difference in the convective blueshift and gravitational redshift of the components amount to just 24 m/s following Eq. 3 of Nidever et al. (2002). Overall, the true error of our determination is likely within 50 m/s.

Having the relative position and velocities on the plane of the sky and the relative velocity along the line of sight, we then derived the family of possible bound solutions as a function of the separation between the components along the line of sight (z) using the approach by Hauser & Marcy (1999) as in Desidera et al. (2011). The results are displayed in Fig. 9.

Critical semimajor axis for dynamical stability of planets around each component, calculated following Holman & Wiegert (1999), are shown in Fig. 10 for the family of possible orbits shown in Fig. 9. This quantity is larger than 40 AU for all the orbits¹. Therefore, the planet candidate is well within the stability boundaries for all possible orbits of the wide binary. The potential astrometric candidate discussed in Sect. 5 is also well within the stability zone. However, if real, its presence should alter the RV difference, the astrometric trends and the mass of one component, with some effects on the family of possible binary orbits.

7. Discussion

The planet candidate around HD106515A, with its minimum mass of about $9.5 M_J$, is one of the few with projected masses close to deuterium burning limit. From available data, we did not detect any additional planets in the system. The high eccentricity of its orbit and the solar-like

¹ At values of $|z|$ larger than 300 the large eccentricity of the binary orbit makes the Holman & Wiegert (1999) equations no longer valid.

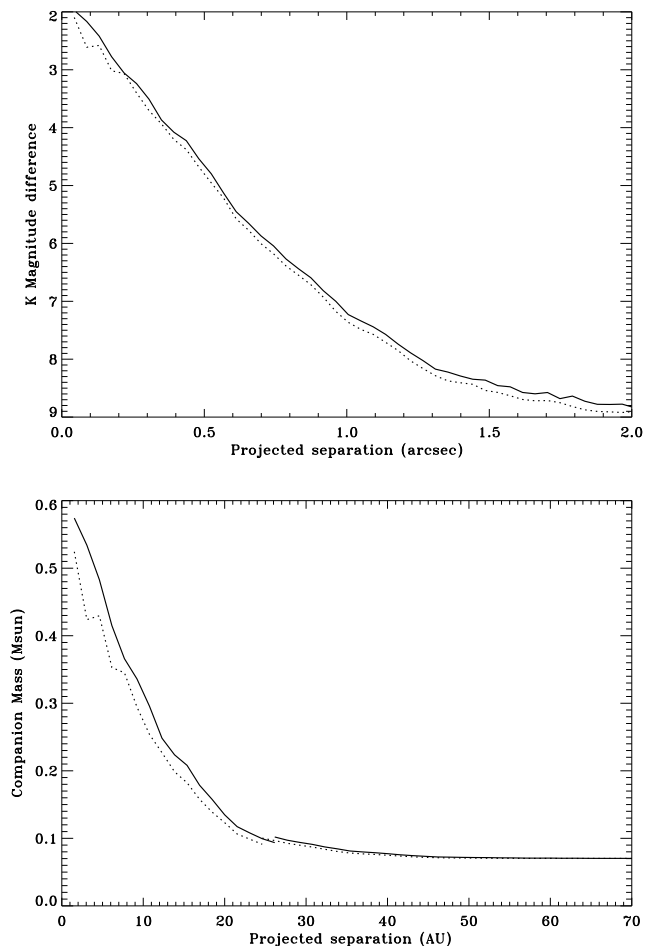


Fig. 8. Detection limits for stellar companions around the components of HD106515 from AdOpt@TNG images. Upper panel: ΔK vs projected separation in arcsec; Lower panel: Companion mass vs projected separation in AU. In both plots continuous line represent detection limits for HD106515A and dotted lines those for HD106515B

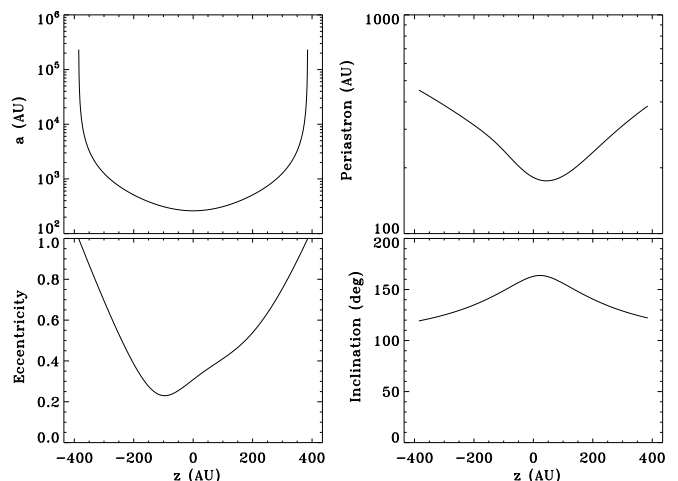


Fig. 9. Possible orbital parameters of the HD106515 system for various separations along the line of sight at present epoch. Top-left: semimajor axis; top-right: periastron of the orbit; bottom-left: eccentricity; bottom-right: inclination.

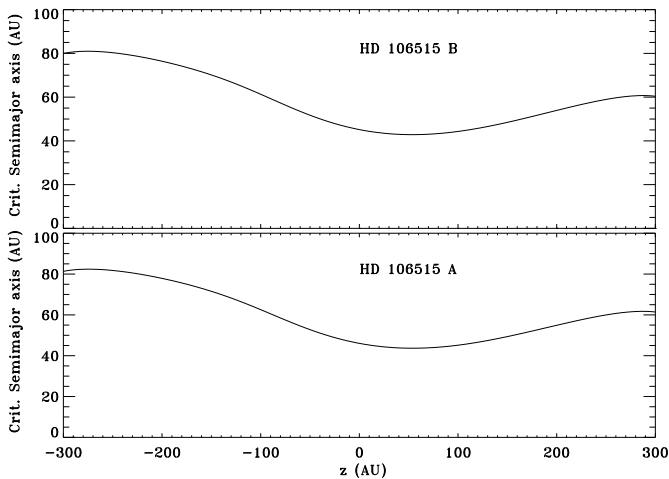


Fig. 10. Critical semimajor axis for dynamical stability for planets around the components of HD106515, for various separations along the line of sight at present epoch and corresponding binary orbit parameters.

metallicity of its parent star are in agreement with the differences in the statistical properties of planets below and above $4 M_J$ found by Ribas & Miralda-Escudé (2007).

The planet host has a stellar companion of similar mass, then HD106515Ab adds to the growing census of exoplanets in multiple systems (Desidera & Barbieri 2007; Roell et al. 2012). The binary separation is quite wide and plausible orbits leave dynamically stable zones up to 40-80 AU around the stars. This suggests a limited impact of the companion on the planet properties but the moderate eccentricity might also be linked to Kozai interactions, which are effective even for widely separated companion considering the old age of the system (Takeda & Rasio 2005). We also found from the analysis of the relative astrometry tentative indication of an additional object with a period of 70 yr. From our data, we can not confirm the reality of this object, that might be a very low mass star, and infer the component around which it should be orbiting.

The presence of a well separated companion with similar properties allowed us to perform a sensitive differential abundance analysis (Desidera et al. 2004, 2006a). The lack of significant metallicity differences between the components extends the previous finding that large alterations of chemical abundances somewhat linked to the presence of planets are not a common event (Desidera et al. 2006a, 2011). There are 8 binary systems with giant planets suitable for the comparison of chemical abundances (HD 106515 and the 7 listed in Table 8 of Desidera et al. 2011). All of them have $\Delta [\text{Fe}/\text{H}] < 0.05$ dex, which is significantly smaller than the typical difference in metallicity between giant planet hosts and nearby field stars ($\Delta [\text{Fe}/\text{H}] \sim 0.25$ dex, see e.g. Fischer & Valenti 2005; Nordström et al. 2004). This supports the primordial origin for the metallicity enhancement of stars with giant planets (Fischer & Valenti 2005).

The binarity of HD106515 represents also a suitable opportunity for the true mass determination HD106515Ab, thanks to the reference provided by HD106515B. The expected astrometric amplitude is of about 1.2 mas for the minimum mass and about 10 mas at stellar/substellar boundary.

From available relative astrometry, the orbital motion of the wide pair is clearly detected. From the analysis of residuals from the long term trend at epochs 1959-1980 where several high-quality data are available we put an upper limit to the mass of the companion of about $0.25 M_\odot$. Much better astrometric precision can be obtained by more recent instrumentation. HD106515 is an ideal target for differential astrometry using AO systems (Hełminiak et al. 2009; Roell et al. 2010) and new interferometric instruments like PRIMA (Quirrenbach et al. 2011). Subsequently, the combination of ground-based radial velocities and Gaia high-precision space-borne astrometric data might prove decisive (e.g., Sozzetti 2011, and references therein).

Therefore, there are very promising perspectives for a true mass determination of the companion of HD106515A in the coming years, then removing the ambiguity due to projection effects. The availability of true masses is relevant for a better understanding of the high-mass tail of the planetary mass function and the transition between planets and brown dwarfs. The direct detection of the companion is instead more challenging even for next generation planet finders as SPHERE or GPI (Beuzit et al. 2010), because of the small projected separations (< 0.2 arcsec) and faint luminosities implied by the old age of the system, unless the orbit is seen nearly pole-on and its mass is significantly larger than the minimum mass.

Acknowledgements. This research has made use of the SIMBAD database, operated at CDS, Strasbourg, France. This research has made use of the Washington Double Star Catalog maintained at the U.S. Naval Observatory. We thank the TNG staff for contributing to the observations and the TNG TAC for generous allocation of observing time. We thank B. Mason for providing the astrometric data collected in the Washington Double Star Catalog. This work was partially funded by PRIN-INAF 2008 and PRIN-INAF 2010.

References

- Arriagada, P. 2011, *ApJ*, 734, 70
 Bakos, G. Á., Howard, A. W., Noyes, R. W., et al. 2009, *ApJ*, 707, 446
 Baraffe, I., Chabrier, G., Barman, T. S., Allard, F., & Hauschildt, P. H. 2003, *A&A*, 402, 701
 Beuzit, J.-L., Boccaletti, A., Feldt, M., et al. 2010, in *Astronomical Society of the Pacific Conference Series*, Vol. 430, *Pathways Towards Habitable Planets*, ed. V. Coudé Du Foresto, D. M. Gelino, & I. Ribas, 231
 Boss, A., Lecavelier des Etangs, A., Mayor, M., et al. 2012, *Transactions of the International Astronomical Union, Series B*, 28, 138
 Bowler, B. P., Liu, M. C., Kraus, A. L., Mann, A. W., & Ireland, M. J. 2011, *ApJ*, 743, 148
 Burrows, A., Hubbard, W. B., Lunine, J. I., & Liebert, J. 2001, *Reviews of Modern Physics*, 73, 719
 Butler, R. P., Wright, J. T., Marcy, G. W., et al. 2006, *ApJ*, 646, 505
 Ceconi, M., Ghedina, A., Bagnara, P., et al. 2006, in *Society of Photo-Optical Instrumentation Engineers (SPIE) Conference Series*, Vol. 6272, *Society of Photo-Optical Instrumentation Engineers (SPIE) Conference Series*
 Chabrier, G., Baraffe, I., Allard, F., & Hauschildt, P. 2000, *ApJ*, 542, 464
 Chauvin, G., Lagrange, A.-M., Zuckerman, B., et al. 2005, *A&A*, 438, L29
 da Silva, L., Girardi, L., Pasquini, L., et al. 2006, *A&A*, 458, 609
 Delfosse, X., Forveille, T., Ségransan, D., et al. 2000, *A&A*, 364, 217
 Desidera, S. & Barbieri, M. 2007, *A&A*, 462, 345
 Desidera, S., Carolo, E., Gratton, R., et al. 2011, *A&A*, 533, A90
 Desidera, S., Gratton, R. G., Lucatello, S., & Claudi, R. U. 2006a, *A&A*, 454, 581
 Desidera, S., Gratton, R. G., Lucatello, S., Claudi, R. U., & Dall, T. H. 2006b, *A&A*, 454, 553

- Desidera, S., Gratton, R. G., Scuderi, S., et al. 2004, *A&A*, 420, 683
- Díaz, R. F., Santerne, A., Sahlmann, J., et al. 2012, *A&A*, 538, A113
- Endl, M., Kürster, M., & Els, S. 2000, *A&A*, 362, 585
- Fischer, D. A. & Valenti, J. 2005, *ApJ*, 622, 1102
- Franz, O. G. e. a. 1963, *Publications of the U.S. Naval Observatory Second Series*, 18, 1
- Gratton, R. G., Bonanno, G., Bruno, P., et al. 2001, *Experimental Astronomy*, 12, 107
- Gray, R. O., Corbally, C. J., Garrison, R. F., McFadden, M. T., & Robinson, P. E. 2003, *AJ*, 126, 2048
- Grether, D. & Lineweaver, C. H. 2006, *ApJ*, 640, 1051
- Hauser, H. M. & Marcy, G. W. 1999, *PASP*, 111, 321
- Heintz, W. D. 1987, *ApJS*, 65, 161
- Helminiak, K. G., Konacki, M., Kulkarni, S. R., & Eisner, J. 2009, *MNRAS*, 400, 406
- Høg, E., Fabricius, C., Makarov, V. V., et al. 2000, *A&A*, 355, L27
- Holman, M. J. & Wiegert, P. A. 1999, *AJ*, 117, 621
- Josties, F. J., Kallarakal, V. V., Douglass, G. G., & Christy, J. W. 1978, *Publications of the U.S. Naval Observatory Second Series*, 24, 7
- Kallarakal, V. V., Lindenblad, I. W., Josties, F. J., et al. 1969, *Publications of the U.S. Naval Observatory Second Series*, 18
- Leggett, S. K., Saumon, D., Marley, M. S., et al. 2012, *ApJ*, 748, 74
- Makarov, V. V. & Kaplan, G. H. 2005, *AJ*, 129, 2420
- Martin, D. C., Fanson, J., Schiminovich, D., et al. 2005, *ApJ*, 619, L1
- Marzari, F. & Weidenschilling, S. J. 2002, *Icarus*, 156, 570
- Mayor, M., Marmier, M., Lovis, C., et al. 2011, *ArXiv e-prints*
- Mordasini, C., Alibert, Y., & Benz, W. 2009, *A&A*, 501, 1139
- Moro-Martín, A., Malhotra, R., Bryden, G., et al. 2010, *ApJ*, 717, 1123
- Nidever, D. L., Marcy, G. W., Butler, R. P., Fischer, D. A., & Vogt, S. S. 2002, *ApJS*, 141, 503
- Nordström, B., Mayor, M., Andersen, J., et al. 2004, *A&A*, 418, 989
- Perryman, M. A. C. & ESA, eds. 1997, *ESA Special Publication*, Vol. 1200, *The HIPPARCOS and TYCHO catalogues. Astrometric and photometric star catalogues derived from the ESA HIPPARCOS Space Astrometry Mission*
- Quirrenbach, A., Geisler, R., Henning, T., et al. 2011, *Research, Science and Technology of Brown Dwarfs and Exoplanets: Proceedings of an International Conference held in Shangai on Occasion of a Total Eclipse of the Sun, Shangai, China*, Edited by E.L. Martin; J. Ge; W. Lin; *EPJ Web of Conferences*, Volume 16, id.07005, 16, 7005
- Reffert, S. & Quirrenbach, A. 2011, *A&A*, 527, A140
- Ribas, I. & Miralda-Escudé, J. 2007, *A&A*, 464, 779
- Roell, T., Neuhäuser, R., & Seifahrt, A. 2010, in *EAS Publications Series*, Vol. 42, *EAS Publications Series*, ed. K. Goździewski, A. Niedzielski, & J. Schneider, 179–186
- Roell, T., Neuhäuser, R., Seifahrt, A., & Mugrauer, M. 2012, *A&A*, 542, A92
- Sahlmann, J., Ségransan, D., Queloz, D., et al. 2011, *A&A*, 525, A95
- Schneider, J., Dédieu, C., Le Sidaner, P., Savalle, R., & Zolotukhin, I. 2011, *A&A*, 532, A79
- Scholz, A., Jayawardhana, R., Muzic, K., et al. 2012, *ArXiv e-prints*
- Skrutskie, M. F., Cutri, R. M., Stiening, R., et al. 2006, *AJ*, 131, 1163
- Sozzetti, A. 2011, in *EAS Publications Series*, Vol. 45, *EAS Publications Series*, 273–278
- Sozzetti, A. & Desidera, S. 2010, *A&A*, 509, A103
- Sumi, T., Kamiya, K., Bennett, D. P., et al. 2011, *Nature*, 473, 349
- Takeda, G. & Rasio, F. A. 2005, *ApJ*, 627, 1001
- van Leeuwen, F. 2007, *A&A*, 474, 653
- Voges, W., Aschenbach, B., Boller, T., et al. 2000, *IAU Circ.*, 7432, 1
- Whitworth, A., Bate, M. R., Nordlund, Å., Reipurth, B., & Zinnecker, H. 2007, *Protostars and Planets V*, 459
- Wright, J. T. 2005, *PASP*, 117, 657
- Zapatero Osorio, M. R., Béjar, V. J. S., Martín, E. L., et al. 2000, *Science*, 290, 103
- Zuckerman, B. & Song, I. 2009, *A&A*, 493, 1149

Table 3. Differential radial velocities of HD 106515 A

HJD -2450000	RV m/s	error m/s
1986.5429	-198.8	2.9
2070.3741	-180.9	1.7
2297.7099	-135.2	3.6
2327.7449	-116.3	3.2
2394.3984	-94.2	2.1
2445.4047	-91.1	2.0
2655.6473	-40.4	3.9
2685.7174	-42.8	3.0
2780.4680	-30.7	2.3
3130.4615	11.5	2.9
3370.7863	24.5	6.7
3373.7381	28.3	2.5
3454.5974	39.8	2.9
3813.5819	75.1	4.7
3898.4270	75.5	2.5
4099.8020	92.0	2.1
4160.6046	95.3	2.8
4221.5300	94.6	2.1
4251.4168	97.6	3.6
4488.7506	107.3	3.2
4545.4910	105.4	2.6
4607.4763	114.7	2.8
4609.4644	119.3	2.3
4849.6782	130.1	3.0
4962.4236	121.2	2.5
5883.7810	-109.7	3.4
5952.7662	-92.9	2.6
5967.6966	-98.9	4.1
6026.5722	-100.2	2.9

Table 4. Differential radial velocities of HD 106515 B

HJD -2450000	RV m/s	error m/s
1986.5544	-19.0	3.2
2070.3879	0.4	1.9
2297.7217	2.6	3.1
2327.7578	5.0	3.5
2394.5070	5.5	2.1
2423.3945	-0.6	2.3
2445.4169	9.1	2.8
2655.6592	0.6	4.5
2685.7307	2.2	3.3
2780.4806	-6.6	2.6
3130.4736	6.8	2.7
3370.7985	11.0	4.9
3373.7496	-12.7	3.8
3454.6096	-1.7	3.7
3813.5692	1.5	5.3
3898.4402	-0.1	2.3
4099.8161	4.5	2.3
4160.6168	-5.9	2.9
4221.5415	-3.8	2.4
4251.4282	-5.1	4.5
4488.7628	7.6	3.8
4545.5030	-12.1	2.8
4607.4885	-9.3	2.8
4609.4782	-4.3	2.3
4849.6896	4.5	3.1
5952.7777	17.2	3.5
5967.7085	16.0	5.1
6026.5845	-13.3	3.4